Advancements in liquid jet technology and X-ray spectroscopy for understanding energy conversion materials during operation

*Torben Reuss[(1)], Sreeju Sreekantan Nair Lalithambika[(1)], Christian David[(2)], Florian Döring[(2,%)], Christian Jooss[(3)], Marcel Risch[(3,&)], Simone Techert [(1,4)]**

(1) Deutsches Elektronen-Synchrotron DESY, Notkestr. 85, 22607 Hamburg, Germany.

(2) Paul Scherrer Institut, Forschungsstrasse 111, 5232 Villigen-PSI, Switzerland.

(3) Institute of Material Physics, Göttingen University, Friedrich Hund Platz 1, 37077 Göttingen, Germany.

(4) Institute for X-ray Physics, Göttingen University, Friedrich Hund Platz 1, 37077 Göttingen, Germany.

*Corresponding author: simone.techert@desy.de

& Present address: Nachwuchsgruppe Gestaltung des Sauerstoffentwicklungsmechanismus Helmholtz-Zentrum Berlin, Hahn-Meitner Platz 1, 14109 Berlin

% Present address: XRnanotech GmbH, Untersiggenthal, Switzerland

CONSPECTUS. Water splitting is intensively studied for sustainable and effective energy storage in green / alternative energy harvesting-storage-release cycles. In this work, we present our recent developments for combining liquid-jet microtechnology with different types of soft X-ray spectroscopy at high flux X-ray sources, in particular developed for studying the oxygen evolution reaction (OER). We are particularly interested in the development of in-situ photon-in / photon-out techniques, such as in-situ Resonant Inelastic X-ray Scattering (RIXS) techniques at high repetition frequency X-ray sources, pointing towards operando capabilities. The pilot catalytic systems we use are perovskites, with the general structure ABO3 with lanthanides or group II elements on the A-site and transition metals on the B-site. Depending on the chemical substitutions of ABO3, their catalytic activity for OER can composition-dependent be tuned.

In this work, we present our in-situ RIXS studies of the manganese L-edge of perovskites during OER. We have developed various X-ray spectroscopy approaches like transmission zone plate-, reflection zone plate- and grating-based emission spectroscopy techniques. Combined with tunable incidence X-ray energies, we yield complementary information about changing (inverse) X-ray absorption features of the perovskites allowing us to deduce element- and oxidation-state-specific chemical monitoring of the catalyst. Adding liquid jet technology, we monitor element- and oxidation-state specific the catalyst with water adsorbate during OER. By comparing the different technical spectroscopy approaches combined with high-repetition frequency experiments at synchrotrons and free-electron lasers, we conclude that the combination of liquid jet with low-resolution zone-plate based X-ray spectroscopy are sufficient for element- and oxidation-state specific chemical monitoring during OER and easy to handle.

For an in-depth study of OER mechanisms, however, including the characterization of catalyst-water adsorbate as their charge transfer properties and specially valence intermediates formed during OER high-resolution spectroscopy tools based on a combination of liquid jets with gratings bear bigger potential since they allow to resolve otherwise overlapping X-ray spectroscopy transitions. Common for all experimental approaches is the

conclusion that without the versatile developments of liquid jets and liquid beam technologies, elaborate experiments such as the highly repetitive experiments at high flux X-ray sources (like synchrotrons or free-electron lasers) would hardly be possible. Such experiments allow a sample refreshment for every single X-ray shot up to 5 MHz repetition frequencies so that it is possible (a) to study X-ray radiation-sensitive samples but also (b) utilize novel types of flux-hungry X-ray spectroscopy tools like photon-in / photon-out X-ray spectroscopy for studying the OER.

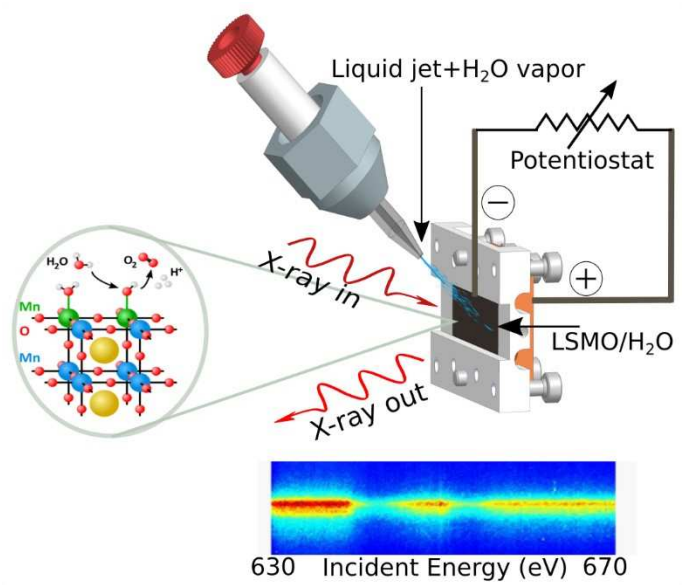

KEY REFERENCES

- Hallmann, J.; Quevedo, W.; Grübel, S.; Rajkovic, I.; Busse, G.; More, R.; Petri, M.; Techert, S. *First steps towards probing chemical reaction dynamics with free-electron laser radiation*. *J. Phys. B: At. Mol. Opt. Phys.* **2010**, 43, 194009-194016.[1] This experimental research papers invents the liquid jet technology to free-electron lasers and demonstrates that the liquid jet can be used in X-ray scattering but also in X-ray spectroscopy setups (allowing to extend to synchrotron experiments, too).
- Busse, P.; Yin, Z.; Mierwaldt, D.; Scholz, J.; Kressdorf, B.; Ronge, E.; Glaser, L.; Deinert, S.; Viefhaus, J.; Jooss, C.; Techert, S.; Risch, M. *Probing the surface of $La_{0.6}Sr_{0.4}MnO_3$ in water vapor by in situ RIXS: interpretation of the fluorescence yields*. *J. Phys. Chem. C* **2020**, 124, 7893-7902.[2] This experimental research paper introduces Resonant Inelastic X-ray Scattering at synchrotron sources for surface studies of the electronic properties of complex catalysts. The studies concentrate on perovkites without / with water vapor confirming former X-ray absorption studies.

- Raabe, S.; Mierwaldt, D.; Zhu, Y.; Blöchl, P.; Jooss, C. *In situ electrochemical electron microscopy study of oxygen evolution activity of doped manganite perovskites*. *Adv. Funct. Mater.* **2012,** 22, 3378-3384.[3] In this work *in situ* electron microscopy is introduced for studying perovskite catalysts for OER. Complementary to *in situ* X-ray spectroscopy, local information about the catalytic activties of the perovskite surface under *in situ* conditions can be derived.

INTRODUCTION

One of the greatest challenges of our current time lies in the systematic research and characterization of chemical reactions that allow the storage and output of energy in a highly efficient manner while conserving natural resources. In the field of the production of so-called "green hydrogen", the hydrogen evolution reaction (HER) as well as the oxygen evolution reaction (OER), i.e., the production of hydrogen and oxygen by water splitting and its back reaction, belong to the most important and currently most studied chemical reactions of water utilization for energy storage and production.[4-13] For the field of high flux X-ray sources, for both synchrotrons and free-electron lasers,[14] this means developing new measurement techniques and methods that provide an alternate and additional view on HER or OER reactions alongside with

existing measurement techniques, leading to improvements in electrochemically and photoelectrochemically active catalysts and their mode of action.

In soft X-ray spectroscopy various ground-breaking techniques have been developed for studying OER focusing on X-ray absorption techniques *in-situ*[15, 16] and *operando*[17-19]. The studies concentrate on detecting the interacting X-rays in absorption mode either by direct transmission absorption experiments or by inverse absorption techniques derived from emission spectra (as explained in the following paragraph). All in all the X-ray spectroscopies allow to monitor element-specific oxidation state changes during OER. In-sight views on hole and electron generations with relation to the band gap properties of the catalytic materials are also possible.

With the presented Resonant Inelastic X-ray Scattering (RIXS) experiments we want to add another precision step by determining intermediate species between the catalyst and the water on the surface of the catalyst. To follow the line of already developed techniques, over the last years we have paid particular attention to the development of time-dependent X-ray methods as time-resolved and ultrafast X-ray diffraction or time-resolved multidimensional soft X-ray spectroscopy for studying chemical reactions beyond X-ray absorption spectroscopy.[1] The development of the flux-hungry X-ray spectroscopy techniques to high resolution (Figure 1A) has become possible since we were technically able to couple the liquid jet with its MHz sample exchange repetition frequency with different photon-in / photon-out X-ray spectrometers. Resonant Inelastic X-ray Scattering (RIXS)[11, 12] is a photon-in / photon-out spectroscopy technique where the outgoing energy of photons scattered on the sample is detected as a function

of incidence X-ray energy. Figure 1A shows such a photon-in / photon-out scheme on a perovskite sample, one of our pilot systems. Essentially RIXS is X-ray emission spectroscopy with tuning the incidence X-ray energies. On an atomistic level, the differences between X-ray absorption spectroscopy (XAS) and RIXS are shown in Figure 1B. Staying with the perovskite example, with soft X-ray spectroscopy, the shown generalized transition diagram applies for the transitions and level involved in RIXS of the oxygen K-edge but also for the transitions and levels involved in the manganese L-edge. For our presented proof-of-concept X-ray spectroscopy studies of the OER, we will concentrate on the X-ray absorption and emission features of the manganese atoms in LSMO, i.e. the manganese L-edge transition features, since we expect their oxidation state changes during the OER. The manganese atoms are highlighted as violet points in the LSMO crystal structure of Figure 1A. Figure 1B depicts the resonant core excitation (XAS) and subsequent RIXS emission. For transition metals, soft x-rays promote the core 2p electrons directly into the 3d frontier states, which is dipole allowed. The subsequent decay from the valence states carries the information crucial for understanding the material's physiochemical properties. We yield information about the population of the electronic states of the investigated material (here a perovskite). Combining it with time-resolved, *in situ* (or even *operando*) X-ray methods allows to deduce changes of the population of the electronic states in a dynamic way. Taking into account that RIXS belongs to the core hole clock spectroscopies (Figure 1B) it is possible to gain information about the highest occupied or lowest unoccupied states of the material, as well as the corresponding band gaps.

SOFT X-RAY EMISSION SPECTROSCOPY DEVELOPMENTS FOR SYNCHROTRONS AND FREE-ELECTRON LASER SOURCES

By tuning the incidence X-ray energy and collecting the X-ray emission (XES) integrally, or – in other word - inverting XES by monitoring particular emission spectroscopy transitions, and tuning the incidence X-ray energies, it is possible to collect partial (when partially integrated, PFY) and total fluorescence yields (TFY) as a function of incidence energies. The spectra collected are comparable to the ones of X-ray absorption spectroscopy in transmission mode.

However, since the X-ray photons are collected in fluorescence and scattering mode and the X-ray penetration depth sets the monitored sample thickness (Figure 1A), the sample thicknesses do not define the collected spectra (i.e. via saturation effects)[1], e.g., when the PFY of the 3s to 3d transition is monitored.[2] It is then possible to study specific selected sheets of layered compositions. An example are layers on target materials, where the spectroscopic properties of the target materials are out of the monitoring window and thus doe not contribute to the background of the collected signals. Furthermore, liquid jets can be added (as another layer), and complex reactions like the OER can be investigated. This finally leads to the possibility of utilizing the full advantages of high flux X-ray sources (time-resolution, high repetition frequencies, flux, brilliance and coherence) allowing for developing high-resolution and multidimensional X-ray spectroscopy tools like X-ray emission spectroscopy (XES) or RIXS.[20-27]

This can enable more detailed investigations of the mechanisms driving the OER. Its technical realization is schematically drawn in Figure 1C and their photographs are shown in Figure 1D. We named this endstation, which was first operational in 2012 in the soft X-ray regime, at that time ChemRIXS endstation.[20-23] In order to reduce background noise on the X-ray spectra, the whole experimental chamber is set to 10^{-3} mbar vacuum which is a challenge for running the liquid jet smoothly. Radiation damage when monitoring chemical reactions with soft X-ray photons is an additional challenge. To avoid or minimize it we have developed a vacuum-compatible liquid jet technology.

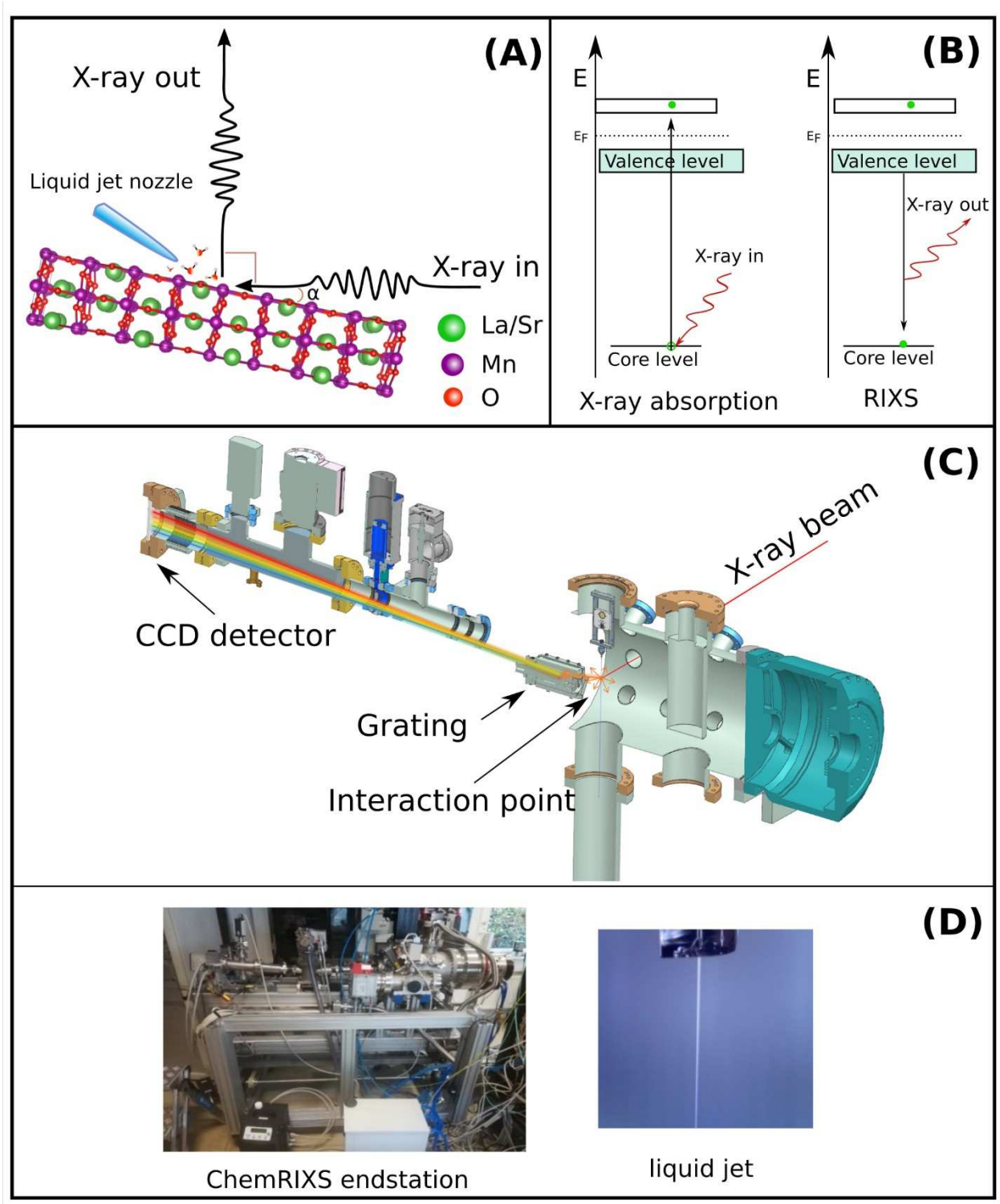

Figure 1: (A) and (B) Principle of Resonant Inelastic X-ray Scattering (RIXS) and difference between X-ray absorption and RIXS excitation schemes. (C) The ChemRIXS chamber. Design

for *in situ* and *operando* studies with ChemRIXS. (D) Photograph of the ChemRIXS chamber and photograph of the liquid jet.

Since the liquid jet technology (Figure 1D) runs up to MHz sample exchange rates, ChemRIXS can be coupled to high-repetition frequency synchrotrons as well as free-electron lasers.[20-23] ChemRIXS has been operated at PETRA-III, FLASH-I, FLASH-II. The liquid jet is used as MHz sample exchange unit in the high-resolution HeisenbergRIXS apparatus at the SCS beamline of the European XFEL.[24] The liquid jet technology can avoid typical soft X-ray radiation damage processes that allow otherwise atypical reaction pathways to occur in electrochemistry - especially important when studying the reactions of water splitting, namely HER and OER.

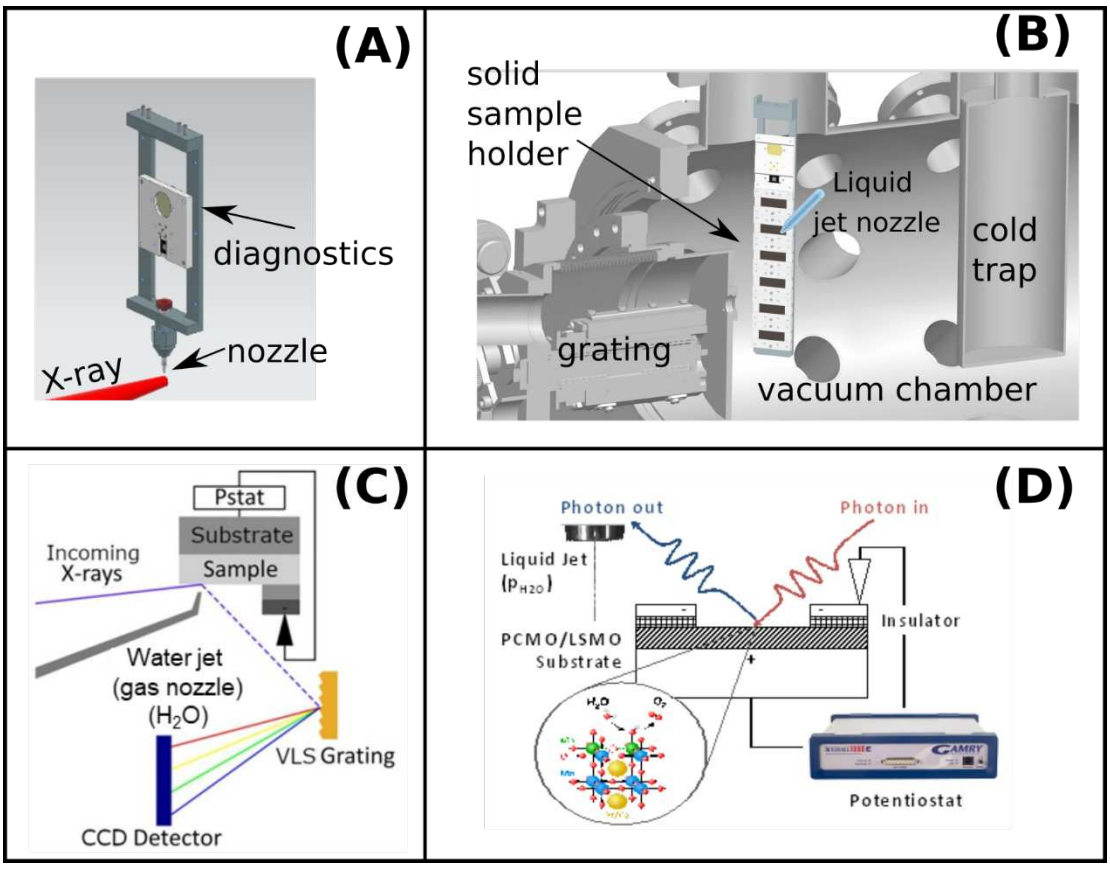

Figure 2: (A) Liquid jet coupling into the ChemRIXS chamber. (B) Liquid jet coupled with surface sensitive (grazing incidence, GI) X-ray geometry for GIRIXS studies. (C) Design of the ChemRIXS-GIRIXS setup for surface / water / liquids studies including a potentiostat for *in situ* (and in future *operando)* GIRIXS studies. (D) Side-view of the setup.

Due to the high-repetition frequency performance of the liquid micro-jet and its compatibility with high-flux X-ray sources, we developed the ChemRIXS chamber for time-resolved, *in situ* and *operando* studies (Figure 2).[2, 20-23] The multi-use liquid jet (Figure 2A) combines calibration tools with the liquid jet. Furthermore, it is combined with solid state samples that are active during the OER catalysis (Figure 2B). For possible *in situ* and *operando* studies the catalysts by

themselves are coupled to a potentiostat (Figure 2C and Figure 2D).[2, 20-23] For *operando* studies additional mass spectrometer monitor the catalytic activities. For time-resolved studies in the case of photocatalyst's studies, a pulsed optical laser has been coupled in.[25-27] *Time-resolved* experiments are reached when external stimuli like pulsed optical laser are coupled in. Various of such proof-of-concept-studies have been performed at FLASH and LCLS for XUV and soft X-ray emission spectroscopy where we determined the electron energy and "real-time movements" (meaning investigating the population changes of electronic states of particular transition energy) in materials, thus contributing to the "film of chemical reactions" from an electron energy, electron orbital and electron distribution point of view for molecular and homogeneous catalytic systems.

Due to the flexible geometric design of the various components, it is possible to run the RIXS spectrometers of ChemRIXS in transmission or reflection or grazing incidence (GI) geometry as GIRIXS.[28, 29] Our *time-resolved*, *in situ* and *operando* XES / RIXS studies can therefore be either bulk or surface sensitive, as shown in Figure 2C and Figure 2D.

Depending on the information about the OER which we want to gather, different X-ray spectrometer types can be combined with liquid microjets in the ChemRIXS chamber.[30-34] The exchangeable, soft X-ray spectrometer units equipped with a transmission zone plate (TZP), a reflection zone plate (RZP) and a classical grating spectrometer (Figure 3). Common for all technical approaches of soft X-ray spectroscopy, the XES and RIXS processes consist of the following steps:

- X-ray beam hits the sample (solid/liquid beam).
- The interaction with the X-rays increases the electron energy in the material/sample under investigation in an element-specific manner.
- The sample emits photons of specific energy.
- Emitted photons hit an optical grating and are separated according to energies.
- Photons separated according to energy hit the detector.
- A spectrum of energies can be measured via the distribution of photons on the detector.

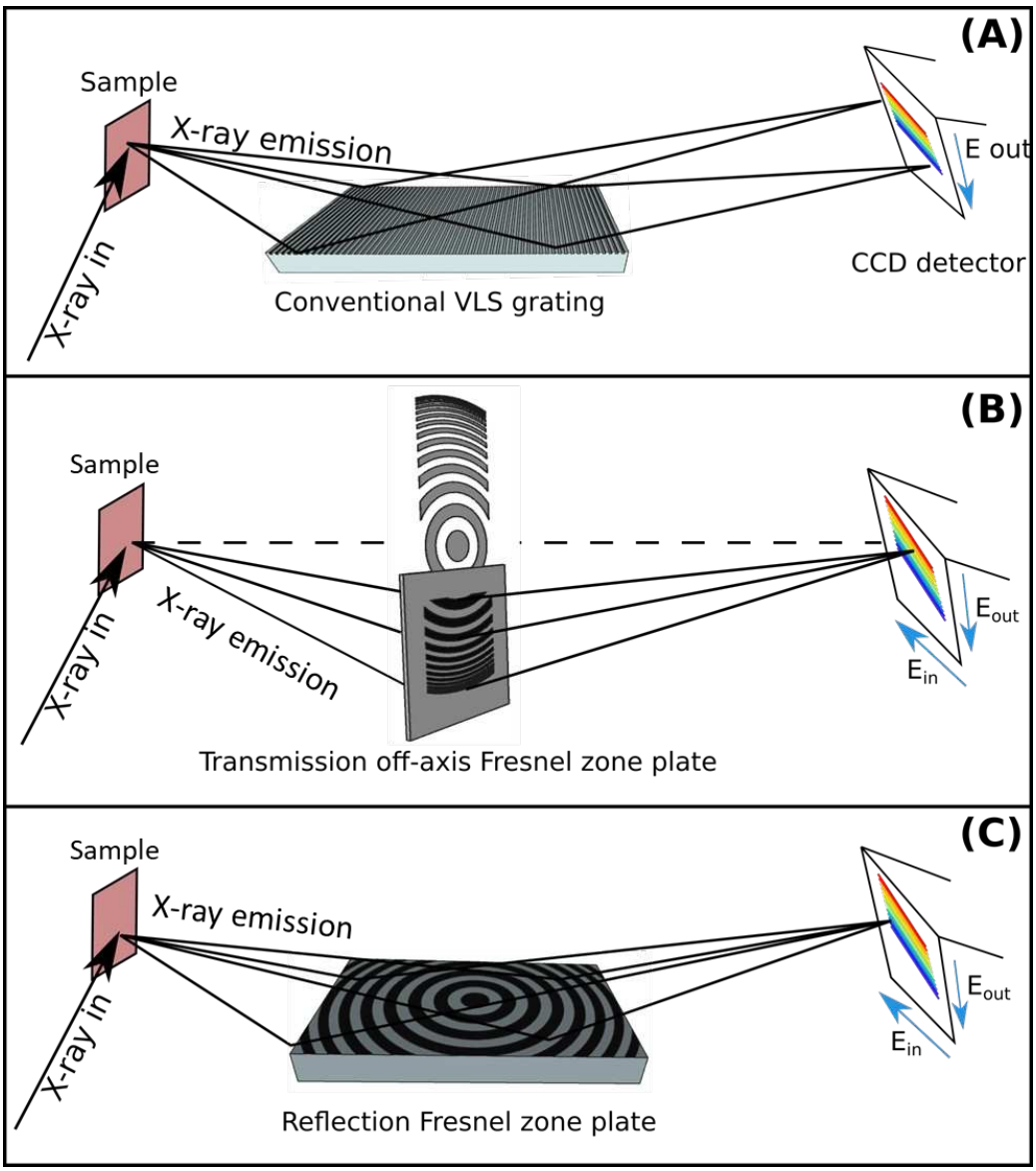

Figure 3: (A) Conventional RIXS detection scheme with a grating. (B) Transmission zone plate for RIXS detection. (C) Reflective zone plate for RIXS detection. All spectrometer can investigate solid state or liquid bulks, or can be operated for grazing incidence recording (GIRIXS). Utilizing the time-structure of the high-flux X-ray photon sources (PETRA-III synchrotron and FLASHI/II free-electron laser) allows for

in situ and operando GIRIXS studies of surfaces with water or other liquids.

In ChemRIXS the liquid jet is either combined with a conventional X-ray grating spectrometer, where the incidence X-ray energy is wavelength-selected by a monochromator of the beamline, and the outgoing X-ray photons are recorded as XES spectra as a function of incidence X-ray energy (Figure 3A). In this way "RIXS maps" can be derived by a stepwise approach of incidence X-ray photon energy tuning, and on the sample scattered outgoing X-ray photon energies recording. This conventional way of high-resolution RIXS maps collection is only efficient and realizable in a reasonable time-window when high-flux X-ray sources with stable photon fluxes are coupled in. Or, when energy resolution issues for the systems investigated are negligible, the recording process can technically be simplified and accelerated by combining the liquid jet with transmission (TZP, Figure 3B) or reflection (RZP, Figure 3C) zone plates where all sample-emitted X-ray photons are locally selected according to their energies and simultaneously recorded on a 2D X-ray detector.

IN SITU STUDIES ON LSMO/H2O/KOH INTERFACES

Depending on the scientific question, with these three different types of spectrometers coupled to liquid microjets, different questions of the OER activity and the OER reaction mechanism are addressed. In the following we will present our comparative studies of *in situ* studies of

$La_{0.6}Sr_{0.4}MnO_3$ (LSMO) in water vapor, LSMO*H_2O, and with alkaline solution, LSMO*H_2O/KOH. LSMO perovskite can either be used as a catalyst for the ORR (oxygen reduction reaction) or the OER. Its perovskite crystal structure is shown in Figure 1A.

Perovskite oxides have the general structure ABO_3, where commonly lanthanides or group II elements are found on the A-site and transition metals on the B-site.[35] Complete or partial substitution of the A-site and/or B-site changes the physicochemical properties of the perovskite oxide often without affecting the perovskite structure significantly. The chemical substitutions on perovskite oxides have been shown to impact its catalytic activity for the OER, making them a good choice for systematic studies.[36-39] Highly crystalline thin films with defined orientation have been insightful model systems studied in water vapor, e.g. by ambient pressure *in situ* soft XAS, [15] *in situ* XPS / XANES,[40] environmental TEM[3, 41-43] or ultrafast time-resolved optical studies.[40] Here we focus on photon-in/photon-out synchrotron spectroscopy using a liquid jet setup.

In this work we will present the scientific results of two types of proof-of-concept-OER-studies on LSMO which resemble two complementary X-ray emission spectroscopy capabilities for *in situ* and *operando* studies:

(i) *The study of the OER under in situ conditions with low-resolution X-ray emission spectroscopy* (Figure 4 and Figure 5): For the qualitative study of the electrochemistry of the bulk catalysts under applied voltage *in situ*, gaseous or liquid jets have been coupled to a low-resolution transmission zone plate spectrometer.

Additionally, we have studied the influence of alkaline solutions on LSMO catalysts properties by analyzing the OER activity of the $La_{0.6}Sr_{0.4}MnO_3$ (LSMO)*H_2O surface reaction with this low-resolution X-ray emission spectroscopy approach. The studies have also been performed adding a mass spectrometer. Since during the experiments no systematic recording has been performed (beyond the confirmation of oxygen production) we will keep the experiments naming them as *in situ* approach rather than *operando* according to the common definitions.

(ii) *The study of the electronic influence of the water adsorbate on the LSMO surface with high-resolution X-ray emission spectroscopy coupled to a liquid jet* (Figure 6 and Figure 7): In the high-resolution X-ray experiment, the electronic properties of the LSMO-water surface has been studied in detail by coupling the liquid jet to a grating spectrometer. This approach allows to diminish radiation damage issues (like the creation of solvated electrons in the water layer) so that the experiment can run with MHz repetition rate. The increase of the rate by 3-5 orders of magnitudes allows for high-resolution electronic structure studies as the X-ray emission / RIXS spectra presented in Figure 7.

In sum, (i) resembles a technical preparation study confirming that LSMO can be studied under *in situ* conditions (or even *operando*) with high flux X-ray sources. It confirms that spectroscopic analysis deduces trends in manganese oxidation states under *in-situ* conditions. The more

sophisticated high-resolution *in situ* X-ray emission studies (ii), which are prepared to deduce radiation damage of the high flux X-ray sources, ca be built in the results obtained in (i) and adds information about the electronic properties of LSMO when water layers are added for the *in situ* experiments.

Both type of soft X-ray spectrometry allow to record the changes in the oxidation state or the element-specific chemical composition of the bulk electrocatalyst or water, of the surface of the electrocatalyst or the water adsorbates. In general, highest surface sensitivity is reached during recording under grazing incidence geometry.

(i) *Study of the LSMO OER under in situ conditions with low-resolution X-ray emission spectroscopy.* For our *in situ* studies we combined TZP X-ray spectroscopy with a potentiostat and monitored the Mn valence and oxidation states of LSMO with water upon voltage stepping. With the TZP-based X-ray spectroscopy the changes of the oxidation states of various elements in LSMO can then be quickly recorded. Integrating in particular the manganese L-edge emission features ($3d \rightarrow 2p_{1/2}$ RIXS) for different applied voltages yields the manganese L-edge partial fluorescence yields as 3d-PFY. For the iPFY signals we applied the same data procedure as been described in the general procedure of integration of the RIXS features of LSMO:[2] we yield the iPFY of the Mn (L-edge) by integrating the region of interest of the O(2p-1s) emission feature and inverting the signal intensity. In the following we will concentrate on the iPFY signals. Changes in (and confirmation of) catalytic activity are additionally monitored by coupling a mass spectrometer to the setup (which is not considered in this work).

On the chemical side, during the OER, water is oxidized to O_2 by the release of electrons, which are given to the LSMO anode surface. At this particular moment of electron admission higher valence intermediate Mn states of Mn^{3+} / Mn^{4+} are formally reduced towards lower valence states by the admission of electrons – to a lower mixed or intermediate valence state $Mn^{2+/3+/4+}$. Note that the occurrence of mixed or intermediate valence states of Mn can be distinguished. Intermediate valence states are present in the metallic phases of LSMO, where 3d electrons in the conduction band are delocalized. This is typically the case for valence states in between of $Mn^{3.2+}$-$Mn^{3.5+}$ in highly crystalline LSMO with low defect density. Mixed valence states are present in semiconducting or insulating phases of LSMO, where electric charge is rather localized and mixed valence states of Mn^{2+}, Mn^{3+} and Mn^{4+} can evolve. This can be e.g. triggered by point defects, change of doping, strain and surface reconstruction. In Figure 4 the iPFY energies haven been set through energy calibrations of reference L-edge Mn absorption spectra of defined Mn oxidation states in various manganese oxides,[15, 35, 45-48] ranging over the manganese valence states of Mn^{2+}, Mn^{3+}, Mn^{2+} / Mn^{3+} and Mn^{4+}. In the current work the beamline and part of the spectrometers have been calibrated on well-defined argon- and xenon-lines of soft X-ray gas detectors.[2, 20] This sets the energy of the spectrometers to 0.1-0.5 eV energy precision. The best energy resolution of the TZP however is about 0.8-1 eV. Independent on the oxidation state we start with, applying Mosley's law yields a +1.6 eV relative shift / oxidation state in our PFY spectra of Figure 4. With the energy resolution of 1 eV in mind, the formal calibration points are the maxima at 639.4 eV for Mn^{2+}, 641.4 eV for Mn^{3+} and 643.2 eV for Mn^{4+}. Additional also

mixed state transitions are assigned to the transitions at 639.6 eV (Mn^{2+} / Mn^{3+}), 640.5 eV (Mn^{2+}), 642 eV (Mn^{2+} / Mn^{3+}) and a 643.8 eV (Mn^{4+}) transition shoulders, also for mixed valences like in Mn_3O_4.[46] The assignment respectively calibration points are marked as vertical blue lines in the PFY spectra of Figure 4.

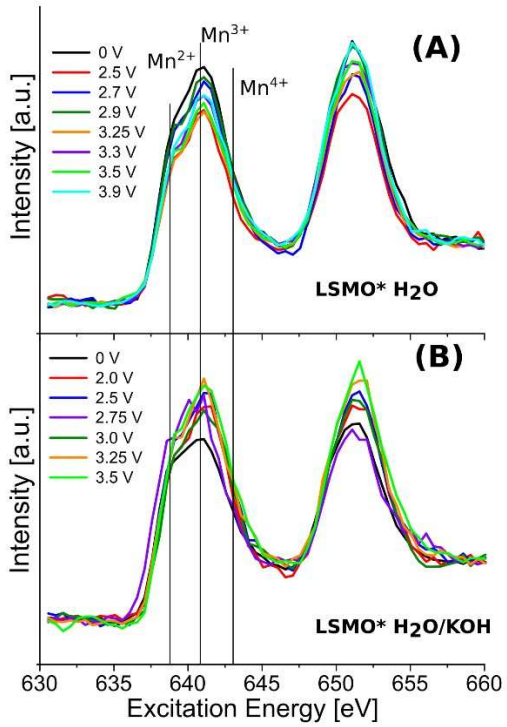

Figure 4: LSMO*H_2O and LSMO*H_2O/KOH surface reaction under voltage steps (vs. ground). (A) *In situ* Mn L-edge iPFY of LSMO*H_2O for varying voltages. (B) *In situ* Mn L-edge iPFY of LSMO*H_2O/KOH for varying voltages. The Mn L-edge iPFYs have been measured with TZP-GIRIXS spectroscopy.

The present OER studies of LSMO (LSMO as anode) under more realistic oxidation conditions reveal also a more precise monitoring of the dynamic LSMO-oxidation state changes (Figure 4) and suggest that a more complex manganese oxidation state mixture is involved in the LSMO-catalyzed OER. Figure 4 also emphasizes that we have already intermediate/mixed valence states reaching from Mn^{2+} to Mn^{4+} in LSMO before the OER – and also on the surface. Since also Mn^{2+} / Mn^{3+} mixed valance transitions are found at around 639.4 eV, and reference is the zero voltage (vs. ground) LSMO form, we interpret the existence of the shoulder and their variation during voltage sweep or surface cover as a change of the manganese valence state towards smaller values, i.e., from $Mn^{+3/+4}$ to Mn^{+3} or even mixed $Mn^{+2/+3}$ states etc. It is safe to state that activating LSMO by the increase of applied voltage leads also to a slight reduction of the surface Mn valence states in LSMO which are not fully recovered by the charge flow back from the bulk and which we will use for the following interpretations as a type of intrinsic LSMO anode feature w/ o water adsorbate and electrolyte around.

Figure 4A shows the *in situ* inverted partial fluorescence yield (iPFY) of LSMO*H_2O and Figure 4B the *in situ* studies of the iPFY of LSMO*H_2O/KOH when the water vapor in the chamber forms a KOH-water mixture with a KOH-covered LSMO film and under voltage sweep. In Figure 4A, the intensity of the iPFY of LSMO*H_2O decreases the first 639 to 643 eV iPFY transition band when the voltage is increased from 0V to 3.9V, and the 2nd iPFY transition band with its maximum at 652.5 eV increases.

For increasing the chemical parameter space of systematic analysis of the OER activity of the electrocatalyst it is important that the RIXS setup includes additional (chemical experimental) degrees of freedom. Therefore the studies have been extended from water to alkaline solution covering LSMO. Alkaline solution can be created by either adding water to the salt covering the LSMO surface, or using mixing units pre-coupled to the nozzle and transfer tube a water in a microjet mixing unit unit that can mix different solution channels and as been described[44, 51] and shown in Figure 1B. When adding alkaline solution to the LSMO surface, at 0 V vs. ground the PFY looks quite similar to the ones of LSMO covered with water without applied voltage potential (Figure 4A). Also here most prominent are the increase of the low-energy transition shoulder of the *in situ* PFY when voltage is ramped up. Within the resolution of the recorded data, the found behavior is quite similar to the ones of LSMO covered with water (Figure 4A) suggesting similar reduction mechanism as been discussed in the case of LSMO*H_2O: when voltage potential is applied, after a specific threshold, again a 639.4 eV transition shoulder appears in the iPFY, due to the formation of lower mixed Mn^{2+} / Mn^{3+} valence states.

With the current spectrometers, we are not sensitive to eventually fully dissolved Mn ions in water or in alkaline solution (with KOH). The phase evolution in different pH and during oxidation have been previously reported for the Mn-based OER catalysts, and they are found to exhibit high structure flexibility that relates to their OER behavior.[52]

Formally, the valence state change of Mn can be monitored by calculating the iPFY intensity ratio of the Mn-L_3 to the Mn-L_2 integral intensity assuming that the Mn-L_3 edge height is reduced

and that other ratios are thus expected for undistorted data. This method has successfully been developed for *in situ* EELS of LSMO for getting a deeper inside into *in situ* studies.[40, 41] Since our PFY spectra are quite distorted (the 3d-PFY even more than the iPFY presented in this work) this analysis can only be seen as a first zero-order approach emphasizing the proof-of-concept of the present study. Figure 5 shows the iPFY intensity ratio of the Mn-L_3 to the Mn-L_2 integral intensity as a function of applied potential. The iPFY ratio Figure 5B is compared to rotating ring-disk studies on the same system (Figure 5A).[49] In Figure 5B, the intensity ratio between the L_2 and L_3 edge are compared for LSMO covered with water, LSMO*H_2O, and LSMO covered with alkaline solution, LSMO*H_2O/KOH. For LSMO*H_2O (red curve) and LSMO*H_2O/KOH (blue curve) a clear tendency to a threshold like behavior has been found.

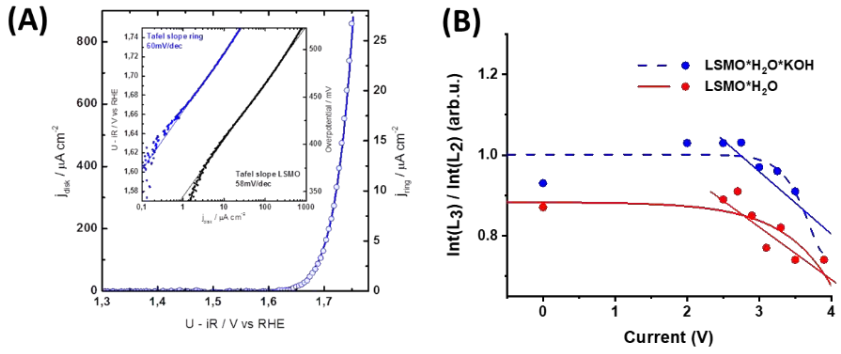

Figure 5: (A) Rotating ring-disk studies of the same LSMO in water system (same doping level, same synthesis approach) emphasizing a voltage threshold around 1.75-1.8 V vs. reversible hydrogen electrode (RHE); inset: LSMO disk and Pt ring detecting oxygen by reduction, big figure: overlay of disk and ring data. (B) iPFY intensity ratio of the Mn-L_3 to the Mn-L_2 integral intensity as a function of applied potential. Red curve/line and red circles:

LSMO*H_2O, blue curve/line and blue circles: LSMO*H_2O/KOH.

In Figure 5B, the ratio onset of LSMO*H_2O is set to 1 for non voltage applied, the ones of LSMO*H_2O/KOH is slightly smaller (0.8). The found voltage-independent abscissa offset decreases in the integral intensity ratio of LSMO*H_2O and LSMO*H_2O/KOH can be explained by the decrease of the emitted photon signal due to the added water / alkaline solution layer and the energy-dependent absorption of the added water / alkaline water layer to LSMO.

For both, LSMO*H_2O and LSMO*H_2O/KOH, a voltage threshold > 2.2 V is found, from where then the ratio monotonically decreases as the voltage increases from 2.2 V to 4 V vs. ground. We hypothesize that the reduction of Mn is due to water/hydroxide oxidation and thus correlate the onset of this reaction with the onset of the OER on LSMO in RRDE laboratory experiments at 1.65-1.7 V vs. RHE, shown in Figure 5A.[49] The RRDE experiments have been performed on the same LSMO system, synthesized in the same way and with the same doping level. The deviations between our found *in situ* studies and the ones from the laboratories can be explained in the following: first, our proof-of-concept studies presented here are technically not as much optimized as the ring electrode experiments, as already the statistics of both experiments suggest. Secondly, our applied voltages are not electronically experimentally referenced as the ring electrode experiments. Third the ratio method utilizing TZP spectroscopy misses some sensitivity (distorted PFY spectra etc.) which add an insensitivity on the ratio scaling (so the ratio changes are detected at higher values than the original ones). Fourth, mechanistic differences may also influence the voltage threshold value since the LSMO sample environment slightly

differ when comparing a ring electrode experiment, and the LSMO water layers produced in this experiment. Overall, Figure 5B emphasizes that it is possible with the explained experiment to monitor *in situ* LSMO activity. However, it also emphasize that more detailed electronic and electronic-structural studies are needed to understand completely the LSMO water coverage:

(ii) The study of the electronic influence of the water adsorbate on the LSMO surface with high-resolution X-ray emission spectroscopy.

When coupling the liquid-jet / LSMO to our high-resolution X-ray emission spectrometer, we can monitor in detail and more sensitive the formation of water layers adsorbed on LSMO. From the TZP-based PFY studies explained in the last paragraph we know that when adding water to the surface, but not applying any voltage potential, the valence states of surface Mn do not reduce to pure Mn^{2+} or Mn^{3+} or intermediate Mn^{2+} / Mn^{3+} valence states. The discussed inconsistencies and normalization furthermore suggest that they may be more modifications in particular on the LSMO surface existent which we have not taken into account yet.

With the grating-based X-ray spectroscopy and utilizing the MHz repetition frequency of the synchrotron RIXS maps of the system can be recorded in an reasonable time. Utilizing the liquid jet reduces the probability of radiation damage. Consequently one RIXS map with the X-ray emission features *versus* the incidence X-ray energy (Figure 6) can be derived which gives a spectral overview over the oxygen K-edge features and the manganese L-edge features (Figure

6) in one map. In the grating experiment, the X-ray transitions between the oxygen K-edge of bulk water and surface water and the ones of the perovskite sublattice in LSMO are well separated allowing to distinguish the partial fluorescence yield of the different oxygen species present in the OER and under the experimental conditions.

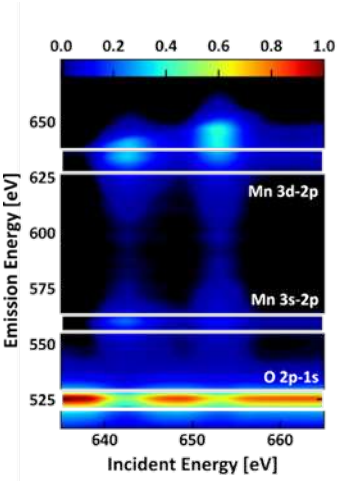

Figure 6: Monitoring the $La_{0.6}Sr_{0.4}MnO_3$ (LSMO)*H_2O responses and the electronic properties of LSMO*H_2O. Utilizing the grating spectrometer, the GIRIXS map are of the Mn L- and O K-edge of LSMO*H_2O are of higher resolution and allow for the investigation of electronic features beyond an elemental and oxidation state investigation.

Figure 7 presents the high-resolution XES spectrum of the manganese L-edge of water-covered LSMO, LSMO*H_2O, recorded with a grating spectrometer. The XES spectrum can directly be

energy-calibrated to the elastic peak (yellow line). Additional different mixed/intermediate Mn^{3+} / Mn^{4+} valence states can be assigned: the resolved transition bands belong to the local (d,d) transition (orange transition bands), the Mn($3d \rightarrow 2p_{1/2}$) fluorescence (grey transition bands) and some Mn^{3+} / Mn^{4+} emission bands in the strong crystal field (cyan transition bands). These transitions have also been found in other LSMO XES studies.[47, 48] Adding water to LSMO, in the XES spectrum of Figure 7 particular for the LSMO*H_2O water adsorbate additional transition bands have been observed not been recorded in our earlier studies studies of dry LSMO in vacuo.[2] We assign these additional (O 2p→ Mn 2p) emission transition bands to charge transfer features from the oxygen atom of the adsorbed water to the manganese atoms of the LSMO surface, abbreviated as $MLCT_{aq}$ and highlighted with orange and purple transition bands in Figure 7. These $MLCT_{aq}$ states alter the activation properties of the surface Mn sites in LSMO even before applying a potential.

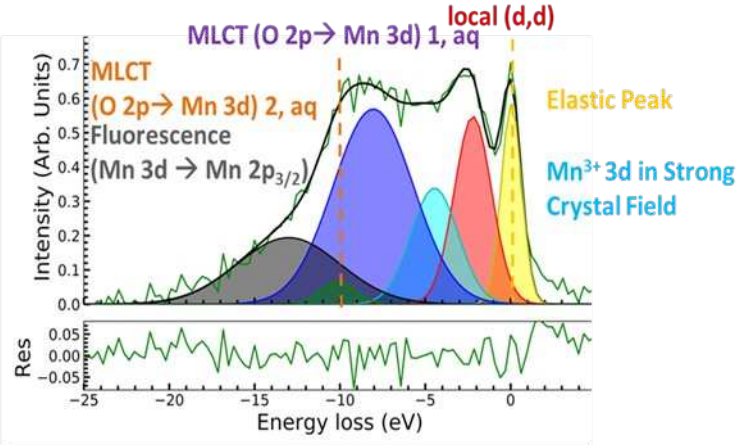

Figure 7: Monitoring the $La_{0.6}Sr_{0.4}MnO_3$ (LSMO)*H_2O responses and the electronic properties of LSMO*H_2O. High-resolution XES of LSMO*H_2O recorded with the grating spectrometer

allows for resolving charge transfer features between solvent and LSMO. The color codes are described in the text. The experiment has been performed combining the liquid-jet technology with RIXS grating spectroscopy. The excitation energy for this spectrum was set to 642.8 eV.

CONCLUSION

We can conclude that the current advances of liquid jet technology, combined with state-of-the-art spectroscopy at high-flux X-ray sources allow the study of the electronic and structural / electronic and mechanistic properties of metastable states as well as very short-living intermediates. Liquid jet technology does not only contribute to time-resolved studies, but can also enhance *in situ* (and *operando*) studies since it reduces the probability of accumulating radiation damage. Depending on the X-ray spectrometer added, qualitative or quantitative chemical analysis, like oxidation state changes or element-specific composition changes can be monitored *in situ*. Due to additional mixing capabilities, liquid jet technologies add further degrees of freedom for the chemical composition. For an in-depth mechanistic study, however, high-resolution X-ray spectroscopy is of advantage. For studying the water-splitting OER electrocatalytic reaction of LSMO perovskite high-resolution grating studies allow to monitor transient charge transfer states, the filling of empty LUMOs of LSMO through the adsorption of water etc. However, all these novel experimental approaches are only possible through the versatile developments of liquid jets and liquid beam technologies.

ASSOCIATED CONTENT

AUTHOR INFORMATION

Corresponding Author

Simone Techert - (1) Photon Science, Notkestr. 85, 22607 Hamburg, Germany. (2) Institute for X-ray Physics, Göttingen University, Friedrich Hund Platz 1, 37077 Göttingen, Germany. Email: simone.techert@desy.de

Present Addresses

Marcel Risch - Nachwuchsgruppe Gestaltung des Sauerstoffentwicklungsmechanismus

Helmholtz-Zentrum Berlin, Hahn-Meitner Platz 1, 14109 Berlin

Florian Döring - XRnanotech GmbH, Untersiggenthal, Switzerland

Author Contributions

The manuscript was written through contributions of all authors. All authors have given approval to the final version of the manuscript.

Funding Sources

The Helmholtz Association is thanked for continuous financial support and DESY for preferred access to X-ray instrumentation (RTIII / POF IV). DESY staff is thanked for their competent help in large scale facility technical and computer support. We gratefully acknowledge funding by the DFG 217133147/SFB 1073 project C02.

Furthermore, the Initiative and Networking Fund of the Helmholtz Association is gratefully acknowledged (programs: HG-Recruitment, HG-Innovation “ECRAPS”, DSF, CMWS, HG-Innovation “FISCOV”).

Financial support by the Deutsche Forschungsgemeinschaft (DFG) within the Collaborative Research Center SFB1073 "*Atomic-scale Control of Energy Conversion*" (project C02), Projektnummer 217133147, are acknowledged.

This work received funding from the EU-H2020 Research and Innovation Program under the Marie Skłodowska-Curie grant agreement No. 701647.

Biographies

Torben Reuß graduated in mechanical engineering from the Hochschule für Angewandte Wissenschaften Hamburg in 2018. He is currently working in the Photon Science division of the Deutsches Elektronen-Synchrotron DESY, Hamburg, where he is in charge of the liquid jet and spectrometer laboratories. He worked on the design and commissioning of various liquid jet systems coupled to X-ray spectrometers, including the next generation of the ChemRIXS endstation and the HeisenbergRIXS experimental station at the SCS beamline of the European XFEL.

Sreeju Sreekantan Nair Lalithambika received his PhD from Freie Universität Berlin in 2019 on the thesis title 'electronic structure of cobalt octahedral complexes in aqueous solution'. He is presently a postdoctoral researcher at the Photon Science division of the Deutsches Elektronen-Synchrotron DESY, Hamburg, studying electronic structure of catalytic materials using soft x-ray spectroscopy.

Christian David is Group Head of X-Ray Nano-Optics at the Laboratory for X-ray Nanoscience and Technologies (LXN) of the Paul Scherrer Institut, Switzerland. His research interest focuses on the micro- and nanofabrication of X-ray optical devices, and to develop new methods based on these optics for applications in X-ray imaging and spectroscopy at synchrotron and X-ray free-electron laser sources.

Florian Döring is the Founder and CEO of XRnanotech, an award-winning Swiss startup company that develops and fabricates nanostructured X-ray optical elements. Bevor starting the company in 2020, he was a postdoctoral researcher at the Paul Scherrer Institut (Switzerland) in the X-ray optics and applications group following a PhD at Georg-August University in Göttingen (Germany).

Christian Jooss is a professor for materials physics at University of Göttingen. His research is focused on complex oxides, i.e. strongly correlated perovskites as an important class of energy materials and using in-situ electron microscopy techniques. He is spokesperson of the CRC 1073 on “atomic scale control of energy conversion”.

Marcel Risch leads the Young Investigator Group NOME at Helmholtz-Zentrum Berlin co-funded by the ERC Starting Grant ME4OER. He earned his PhD from Free University Berlin and performed interdisciplinary postdoctoral work at MIT. Marcel is enthusiastic about the knowledge-guided design of electrocatalysts for oxygen and nitrogen electrocatalysis for sustainable fuels such as green hydrogen harnessing insights from innovative operando experiments.

Simone Techert is Leading Scientist within the Photon Science division of the Deutsches Elektronen-Synchrotron DESY, Hamburg, and Professor for Ultrafast X-ray Science at Göttingen University. Her research concentrates on kinetic and time-resolved (ultrafast, *in situ*, *operando*) X-ray methods development for complex chemical systems and reaction studies (like water splitting or photovoltaics) and the investigation of the electronic and structural properties and dynamics of (sustainable) functional materials.

ACKNOWLEDGMENT

The authors thank in particular Jens Viefhaus, Leif Glaser and Katharina Kubicek for technical support of the new results presented in this manuscript. Zhong Yin is thanked for his technical support of ChemRIXS for the OER studies. Max Baumung and Philipp Busse are thanked for their contribution in integrating collected RIXS spectra. We acknowledge DESY (Hamburg, Germany), a member of the Helmholtz Association HGF, for the provision of experimental facilities. Parts of the reported research were carried out at PETRA III, Beamline **P04** and FLASH (Beamlines BL1, BL2, BL3 / CAMP) and FLASH-II (FL24). The involved X-ray research teams as well as the optical laser teams are acknowledged. Beamtime was allocated for proposals No I-2051059, 04/2006 to I-20220013, 04/2022, for a complete list of proposals see data base.

The Helmholtz Association is thanked for continuous financial support and DESY for preferred access to X-ray instrumentation (RTIII / POF IV). DESY staff is thanked for their competent help in large scale facility technical and computer support.

REFERENCES

1. Hallmann, J.; Quevedo, W.; Grübel, S.; Rajkovic, I.; Busse, G.; More, R.; Petri, M.; Techert, S. *First steps towards probing chemical reaction dynamics with free-electron laser radiation*. *J. Phys. B: At. Mol. Opt. Phys.* **2010**, 43, 194009-194016.

2. Busse, P.; Yin, Z.; Mierwaldt, D.; Scholz, J.; Kressdorf, B.; Ronge, E.; Glaser, L.; Deinert, S.; Viefhaus, J.; Jooss, C.; Techert, S.; Risch, M. *Probing the surface of $La_{0.6}Sr_{0.4}MnO_3$ in water vapor by in situ RIXS: interpretation of the fluorescence yields*. *J. Phys. Chem. C* **2020***,* 124, 7893-7902.

3. Raabe, S.; Mierwaldt, D.; Zhu, Y.; Blöchl, P.; Jooss, C. *In situ electrochemical electron microscopy study of oxygen evolution activity of doped manganite perovskites*. *Adv. Funct. Mater.* **2012,** 22, 3378-3384.

4. Man, I.; Su, H.; Calle-Vallejo, F.; Hansen, H.; Martínez, J.; Inoglu, N.; Kitchin, J.; Jaramillo, T.; Nørskov, J.; Rossmeisl, J. *Universality in oxygen evolution electrocatalysis on oxide surfaces. Chem. Cat. Chem.* **2011**, 3, 1159-1165.

5. Armstrong, F. *Why did Nature choose manganese to make oxygen? Phil. Trans. R. Soc. B* **2008**, 363, 1263 – 1270.

6. Gono, P. Pasquarello, A. *Oxygen evolution reaction: bifunctional mechanism breaking the linear scaling relationship. J. Chem. Phys.* **2020**, 152, 1047121-1047128.

7. Guan, D.; Ryu, D.; Hu, Z.; Zhou, J.; Dong, C.; Huang, Y.; Zhang, K.; Zhong, Y.; Komarek, A.; Zhu, M.; Wu, X.; Pao, C.; Chang, C.; Lin, H.; Chen, C.; Zhou, W; Shao, Z. *Utilizing ion leaching effects for achieving high oxygen-evolving performance on hybrid nanocomposite with self-optimized behaviors. Nat. Comm.* **2020**, 11, 3376.

8. Song, J.; Wei, C.; Huang, Z.; Liu, C.; Zeng, L.; Wang, X.; Xu, Z. *A review on fundamentals for designing oxygen evolution electrocatalysts. Chem. Soc. Rev.* **2020**, 49, 2196.

9. Rossmeisl, J.; Qu, Z. W.; Zhu, Z.; Kroes, G. J.; Norskov, J. K. *Electrolysis of water on oxide surfaces. J. Electroanal. Chem.* **2007**, 607, 83.

10. Conway, B. E.; Salomon, M. *Electrochemical reaction orders: applications to the hydrogen- and oxygen-evolution reactions. Electrochim. Acta* **1964**, 9, 1599.

11. Kobussen, A. G. C.; Broers, G. H. *The Oxygen Evolution on $La_{0.5}Ba_{0.5}CoO_3$: Theoretical impedance behaviour for a multi-step mechanism involving two adsorbates. J. Electroanal. Chem.* **1981**, 126, 221–240.

12. Grimaud, A.; May, K.; Carlton, E.; Lee, Y.; Risch, M.; Hong, W.; Zhou, J.; Shao-Horn, Y. *Double perovskites as a family of highly active catalysts for oxygen evolution in alkaline solution. Nat. Comm.* **2013**, 4, 2439-2442.

13. Rossmeisl, J.; Logadottir, A.; Norskov, J. K. *Electrolysis of water on (oxidized) metal surfaces. Chem. Phys.* **2005**, 319, 178-184.

14. See the different technical design reports of current and future high-flux X-ray sources including: SSRL: https://www-ssrl.slac.stanford.edu/ (accessed 2022-12-06); LCLS: https://lcls.slac.stanford.edu/ (accessed 2022-12-06); ALS: https://als.lbl.gov/ (accessed 2022-12-06); APS: https://www.anl.gov/ (accessed 2022-12-06); CHESS: https://www.chess.cornell.edu/ (accessed 2022-12-06); NSLS II: https://www.bnl.gov/nsls2/ (accessed 2022-12-06); LNLS-

Sirius: https://lnls.cnpem.br/home/ (accessed 2022-12-06); SACLA: https://sacla.xfel.jp/?p=312&lang=en (accessed 2022-12-06); Spring-8: http://www.spring8.or.jp/en/ (accessed 2022-12-06), NanoTerasu: https://www.nanoterasu.jp/ (accessed 2022-12-06); HZB: https://www.helmholtz-berlin.de/forschung/quellen/bessy/index_de.html (accessed 2022-12-06); PETRA III: https://photon-science.desy.de/ (accessed 2022-12-06); PETRA IV: https://www.desy.de/research/facilities__projects/petra_iv/index_eng.html (accessed 2022-12-06); FLASH: https://flash.desy.de/ (accessed 2022-12-06), European XFEL: https://www.xfel.eu/ (accessed 2022-12-06); MAXLAB IV: https://www.maxiv.lu.se/ (accessed 2022-12-06); ESRF-EBS: https://www.esrf.fr/about/upgrade (accessed 2022-12-06); SOLEIL: https://www.synchrotron-soleil.fr/en (accessed 2022-12-06); ALBA: https://www.cells.es/en/ (accessed 2022-12-06); Elettra: https://www.elettra.eu/ (accessed 2022-12-06); FERMI: https://www.elettra.eu/lightsources/fermi.html (accessed 2022-12-06) and the described research projects therein.

15. Risch, M.; Stoerzinger, K.; Han, B.; Regier, T.; Peak, D.; Sayed, S.; Wei, C.; Xu, Z.; Shao-Horn, Y. *Redox processes of manganese oxide in catalyzing oxygen evolution and reduction: An in situ soft X-ray absorption spectroscopy study*. *J. Phys. Chem. C* **2017**, 121, 33, 17682–17692.

16. Xi, L.; Schwanke, C.; Xiao, J.; Abdi, F.; Zaharieva, I.; Lange, K. *In situ L-Edge XAS study of a manganese oxide water oxidation catalyst*, *J. Phys. Chem. C* **2017**, 121, 22, 12003–12009.

17. Braun, A.; Sivula, K.; Bora, D.; Zhu, J.; Zhang, L.; Grätzel, M.; Guo, J.; Constable, E.; *Direct observation of two electron holes in a hematite photoanode during photoelectrochemical water splitting, J. Phys. Chem. C* 2012, 116, 32, 16870–16875.

18. Al Samarai, M.; Hahn, A.; Askari, A.; Cui, Y.; Yamazoe, K.; Miyawaki, J.; Harada, Y.; Rüdiger, O.; DeBeer, S. *Elucidation of structure–activity correlations in a nickel manganese*

oxide Oxygen evolution reaction catalyst by operando Ni L-edge X-ray absorption spectroscopy and 2p3d resonant inelastic X-ray scattering, A*CS Appl. Mater. Interfaces* **2019**, 11, 42, 38595–38605.

19. Drevon, D.; Görlin, M.; Chernev, P.; Xi, L.; Dau, H.; Lange, K. *Uncovering The role of oxygen in Ni-Fe(O_xH_y) electrocatalysts using in situ soft X-ray absorption spectroscopy during the oxygen evolution reaction, Sci. Rep.* **2019**, 9, 1532-1 – 1532-4.

20. Rajkovic, I.; Hallmann, J.; Grübel, S.; More, R.; Quevedo, W.; Petri, M.; Techert, S. *Development of a multipurpose vacuum chamber for serial optical and diffraction experiments with free-electron laser radiation. Rev. Sci. Instr.* **2010**, 81, 045105-1-6.

21. Yin, Z.; Rajkovic, I.; Raiser, D.; Scholz, M.; Techert, S. *Experimental setup for high resolution X-ray spectroscopy of solids and liquid samples. Proc. SPIE 8849*, *X-ray Lasers and Coherent X-ray Sources: Development and Applications X* **2013**, 88490I.

22. Yin, Z.; Peters, B.; Hahn, U.; Agaker, M.; Hage, A.; Scholz, F.; Reinninger, R.; Siewert, F.; Nordgren, J.; Viefhaus, J.; Techert, S. *A new compact VUV-Spectrometer for RIXS studies at DESY. Rev. Sci. Instr.* **2015***,* 86, 093109-1-5.

23. Yin, Z.; Peters, H.; Hahn, U.; Gonschior, J.; Mierwaldt, D.; Rajkovic, I.; Viefhaus, J.; C. Jooss, C.; Techert, S. *An endstation for resonant inelastic X-ray scattering studies of solid and liquid samples. J. Synchrotron Rad.* **2017**, 24, 302-306.

24. hRIXS Consortium (A. Föhlisch ed.): Technical Design Report of the Heisenberg RIXS@EuropeanXFEL (hRIXS) Endstation as to be operated at the "Spectroscopy and Coherent Scattering (SCS) instrument" at the European XFEL"; https://www.xfel.eu/facility/instruments/scs/index_eng.html **(**accessed 2022-12-06).

25. Quevedo, W.; Busse, G.; Hallmann, J.; More, R.; Petri, M.; Krasniqi, F.; Rudenko, A.; Tschentscher, Th.; Foehlisch, A.; Pietsch, A.; Beye, M.; Stojanovic, N.; Düsterer, S.; Treusch, R.; Tolkiehn, M.; Mann, K.; Peth, C.; Techert, S.; Rajkovic, I. *Ultrafast time dynamics studies of periodic lattices under free-electron laser radiation. J. Appl. Phys.* **2012**, 12, 093519-5.

26. Kunnus, K.; Rajkovic, I.; Schreck, S.; Quevedo, W.; Eckert, S.; Beye, M.; Suljoti, E.; Weniger, C.; Kalus, C.; Grübel, S.; Scholz, M.; Nordlund, D.; Zhang, W.; Hartsock, R. W.; Gaffney, K. J.; Schlotter, W. F.; Turner, J. J.; Kennedy, B.; Hennies, F.; Techert, S.; Wernet, P.; Föhlisch, A. *A setup for resonant inelastic soft X-ray scattering on liquids at free-electron laser light sources. Rev. Sci. Instrum.* **2012***,* 83, 123109-17.

27. Wernet, P.; Kunnus, K.; Josefsson, I.; Rajkovic, I.; Quevedo, W.; Beye, M.; Schreck, S.; Grübel, S.; Scholz, M.; Nordlund, D.; Zhang, W.; Hartsock, R. W.; Schlotter, W. F.; Turner, J. J.; Kennedy, B.; Hennies, F.; de Groot, F. M. F.; Gaffney, K. J.; Techert, S.; Odelius, M.; Föhlisch, A. *Orbital-specific mapping of the ligand exchange dynamics of $Fe(CO)_5$ in solution. Nature* **2015**, 520 (7545), 78-81.

28. Yin, Z.; Busse, P.; Mierwaldt, D.; Jooss, C.; Techert, S.; *Report of the ChemGIRIXS@DESY End-station,* commissioned at the PETRA III synchrotron **2017**.

29. Kaan, A.; Techert, S.; *Report of the ChemGIRIXS@DESY Endstation*, commissioned at the FLASH free-electron laser **2019**.

30. Yin, Z.; Rehanek, J.; Löchel, H.; Braig, C.; Buck, J.; Firsov, A.; Viefhaus, J.; Erko, A.; Techert, S.; *A Highly efficient soft X-ray spectrometer based on reflection zone plate for resonant inelastic X-ray scattering measurements. Opt. Expr.* **2017***,* 25 (10), 10984.

31. Marschall, F.; Yin, Z.; Beye, M.; Buck, J.; Döring, F.; Guzenko, V.; Kubicek, K.; Rehanek, J.;Raiser, D.; Rösner, B.; Rothkirch, A.; Thekku Veedu, S.; Viefhaus, J.; David, C.; Techert, S.;

Transmission zone plates as analyzers for efficient parallel 2D RIXS-mapping. Nat. Sci. Rep. **2017***,* 7(1)*,* 8849-8857.

32. Yin, Z.; Löchel, H.; Rehanek, J.; Goy, C.; Kalinin, A.; Schottelius, A.; Trinter, F.; Miedema, P.; Jain, A.; Valerio, J.; Busse, P.; Lehmkühler, F.; Möller, J.; Grübel, G.; Madsen, A.; Viefhaus, J.; Grisenti, R.; Beye, M.; Erko, A.; Techert, S. *X-ray spectroscopy with variable line spacing based on reflection zone plate optics. Opt. Lett.* **2018***,* 43 (18)*,* 4390 - 4393.

33. Döring, F.; Rösner, B.; Beye, M.; Busse, P.; Kubiček, K.; Glaser, L.; Miedema, P.; Soltau, J.; Raiser, D.; Guzenko, V.; Szabadics, L.; Kochanneck, L.; Baumung, M.; Buck, J.; Jooss, C.; Techert, S.; David, C.; *A zone-plate-based two-color spectrometer for indirect X-ray absorption spectroscopy. J. Synchr. Rad.* **2019***,* 26 (4), 1266–1271.

34. Yin, Z.; Inhester, L.; Thekku Veedu, S.; Quevedo, W.; Pietzsch, A.; Wernet, P.; Groenhof, G.; Alexander Föhlisch, A.; Grubmüller, H.; Techert, S., *Cationic and anionic impact on the electronic structure of liquid water. J. Phys. Chem. Lett.* **2017***,* 8, 3759-3764.

35. Breternitz, J.; Schorr, S. *What defines a perovskite? Adv. Energy Mater.* **2018**, 8 (34), 1802366.

36. Antipin, D.; Risch; M.; *Trends of epitaxial perovskite oxide films catalyzing the oxygen evolution reaction in alkaline media*. *J. Phys. Energy* **2020,** 2032003-2032005.

37. Scholz, J.; Risch, M.; Wartner, G.; Luderer, C.; Roddatis, V.; Jooss, C. *Tayloring the oxygen evolution activity and stability using defect chemistry*. *Catal.* **2017**, 7, 1391-1410.

38. Stoerzinger, K.; Hong, W.; Azimi, G.; Giordano, L.; Lee, Y.; Crumlin, E.; Biegalski, M.; Bluhm, H.; Varanasi, K.; Shao-Horn, Y. Reactivity of perovskites with water: role of hydroxylation in wetting and implications for oxygen electrocatalysis. *J. Phys. Chem. C* **2015**, 119, 32, 18504–18512.

39. Forslund, R.; Hardin, W.; Rong, X.; Abakumov, A.; Filimonov, D.; Alexander, C.; Tyler Mefford, J.; Iyer, H.; Kolpak, A.; Johnston, K.; Stevenson, K. *Exceptional electrocatalytic oxygen evolution via tunable charge transfer interactions in* $La_{0.5}Sr_{1.5}Ni_{1-x}Fe_xO_{4\pm\delta}$ *Ruddlesden-Popper oxide. Nat. Comm.* **2018**, 9, 3150-3156.

40. Mierwaldt, D.; Mildner, S.; Arrigo, R.; Knop-Gericke, A.; Franke, E.; Blumenstein, A.; Hoffmann, J.; Jooss, C. *In situ XANES/XPS investigation of doped manganese perovskite catalysts. Catal.* **2014**, 4, 129–145.

41. Raabe, S.; Mierwaldt, D.; Ciston, J.; Uijttewaal, M.; Stein, H.; Hoffmann, H.; Zhu, Y.; Blöchl, P.; Jooss, C. *In situ electrochemical electron microscopy study of oxygen evolution activity of doped manganite perovskites. Adv. Funct. Mat.* **2012**, 22 (16), 3378-3388.

42. Lole, G.; Roddatis, V.; Ross, U.; Risch, M.; Meyer, T.; Rump, L.; Geppert, J.; Wartner, G.; Blöchl, P.; Jooss, C. *Dynamic observation of Mn-adatom mobility at perovskite oxide catalyst interfaces to water*. *Comm. Mat.* **2020**, 68, 1.

43. Roddatis, V.; Lole, G.; Jooss, C. *In situ preparation of Pr1-xCaxMnO3 and La1-xSrxMnO3 catalysts surface for high-resolution environmental transmission electron microscopy*. Catalysts **2019**, 9, 751-755.

44. Raiser, D.; Mildner, S.; Sotoudeh, M.; Blöchl, P.; Techert, S.; Jooss, C. *Evolution of hot polaron states with a nanosecond lifetime in a manganite. Adv. Energy Mat.* **2017**, 1, 1-9.

45. Risch, M.; Stoerzinger, K.; Regier, T.; Peak, D.; Sayed, S.; Shao-Horn, Y. *Reversibility of Ferri-/ Ferrocyanide Redox during Operando Soft X-ray Spectroscopy. J. Phys. Chem. C* **2015**, 119, 33, 18903–18910.

46. Gilbert, B.; Frazer, B. H.; Belz, A.; Conrad, P. G.; Nealson, K. H.; Haskel, D.; Lang, J. C.; Srajer, G.; De Stasio, G. *Multiple scattering calculations of bonding and X-ray absorption spectroscopy of manganese oxides*. *J. Phys. Chem. A* **2010**, 107(16), 44-48.

47. Kuepper, K.; Klingeler, R.; Reutler, P.; Büchner, B.; Neumann, M.; *Excited and ground state properties of LaSrMnO4 : A combined x-ray spectroscopic study*, *Phys. Rev. B* **2006**, 74**,** 115103-1-11513-7.

48. Agui, A.; Butorin, S.; Kaambre, T.; Sathe, C.; Saitoh, T.; Moritomo, Y.; Nordgren, J.; *Resonant Mn L Emission Spectra of Layered Manganite La1:2Sr1:8Mn2O7, J. Phys. Soc. Jpn.* **2005**, 74 (6), 1772-1776.

49. Scholz, J.; Risch, M; Stoerzinger, K.; Wartner, G.; Shao-Horn, Y.; C Jooss, C. *Rotating ring–disk electrode study of oxygen evolution at a perovskite surface: correlating activity to manganese concentration. J. Phys. Chem. C* **2016**, 120 (49), 27746-27756.

50. Jain, R.; Burg, T.; Petri, M.; Kirschbaum, S.; Feindt, H.; Steltenkamp, S.; S. Sonnenkalb, S.; Becker, S.; Griesinger, C.; Menzel, A.; Techert, S. *Efficient microchannel device for scattering experiments with high flux X-ray sources and their perspective towards application in neutron scattering science. Eur. Phys. J. E* **2013**, 36, 109-118.

51. Jain, J.; Techert, S. *Time-resolved and in situ X-ray scattering methods beyond photoactivation: utilizing high-flux X-ray sources for the study of ubiquitious non-photon active proteins. Special Issue: "Synchrotron Applications in Life Science", Prot. Pept. Lett.* **2016**, 23, 01-22.

52. An, H.; Chen, Z.; Yang, J.; Feng, Z.; Wang, X.; Fan, F.; Li, C. *An Operando-Raman study on oxygen evolution of manganese oxides: Roles of phase composition and amorphization, J. Catal.* **2018**, 367, 53-61.